

Tensile Properties and Microstructure of SiC Nanoparticle–Reinforced Mg-4Zn Alloy Fabricated by Ultrasonic Cavitation–Based Solidification Processing

G. CAO, J. KOBLSKA, H. KONISHI, and X. LI

Magnesium, the lightest structural metal, is of significance to improve energy efficiency in various applications. Mg-4Zn/1.5 pct SiC nanocomposites were successfully fabricated by ultrasonic cavitation–based dispersion of SiC nanoparticles in Mg-4Zn alloy melt. As compared to the Mg-4Zn magnesium alloy matrix, the tensile properties including tensile strength, yield strength, and ductility of the Mg-4Zn/1.5 pct SiC nanocomposites were improved significantly. In the microstructure of Mg-4Zn/1.5 pct SiC nanocomposites, there are still some SiC microclusters. However, in areas outside the microclusters, the SiC nanoparticles were dispersed very well. Transmission electron microscopy (TEM) study of the interface between the SiC nanoparticles and Mg-4Zn magnesium alloy matrix suggested that SiC nanoparticles bonded well with Mg without forming an intermediate phase.

DOI: 10.1007/s11661-007-9453-6

© The Minerals, Metals & Materials Society and ASM International 2008

I. INTRODUCTION

MAGNESIUM-BASED metal matrix composites (MMCs) have been extensively studied as an attractive choice for aerospace and automotive applications due to their low density and superior specific properties including strength, stiffness, and creep resistance. Xi *et al.*^[1] studied the Ti-6Al-4V particulate (TAp)–reinforced magnesium matrix composite, which is fabricated *via* the powder metallurgy (PM) route. It was found that the tensile strength of the composite was markedly higher than that of the unreinforced magnesium alloy. Xi *et al.*^[2] also studied the SiC whisker-reinforced MB15 magnesium matrix composites by PM and found that the mechanical properties of the SiCw/MB15 composite were significantly influenced by the powder-mixing methods of PM. Li *et al.*^[3] studied the hot deformation behavior of SiC whisker–reinforced AZ91 magnesium matrix composites in compression. It was found that the microstructure evolutions involved the movement of SiC whiskers and the changes of the matrix, and the rotation and the broken SiC whiskers, tended to be obvious with the increasing strain, and also a high density of dislocation was observed in the AZ91 matrix at the initial stage of compression (1 pct). Oqinuma *et al.*^[4] studied the magnesium composite alloy with Mg₂Si dispersoids. The Mg₂Si compounds were formed in the solid state by spark plasma sintering Mg-33.33 mol pct Si. Mg₂Si particles cause pores at primary particle boundaries, and sinterability between magnesium alloy

powders was poor due to their thermal stability. Jiang *et al.*^[5] studied that magnesium metal matrix composites (MMCs) reinforced with B₄C particulates fabricated by PM. The hardness and wear resistance of the composites were higher than those of as-cast Mg ingots and increased with an increasing amount of B₄C particulates from 10 to 20 vol pct. Zhang *et al.*^[6] studied the carbon nanotube–reinforced magnesium metal matrix composite by stirring the carbon nanotube into magnesium melts. It was found that the carbon nanotube, especially a chemical nickel-plated one, is excellent in strengthening the magnesium matrix. The structure of magnesium was refined. The tensile strength and elongation of the composites were also improved. Ma *et al.*^[7] studied the TiB₂-TiC particle–reinforced AZ91D alloy. The results showed that the hardness and wear resistance of the composites were higher than those of the unreinforced AZ91 alloy. Pahutova *et al.*^[8] studied the creep resistance of squeeze-cast AZ91 and QE22 magnesium alloys reinforced by 20 vol pct Al₂O₃ short fibers and showed that the creep resistance of reinforced materials was considerably improved compared to the monolithic alloys. Ye *et al.*^[9] reviewed the recent progress in magnesium matrix composites. The conventional methods such as stir casting, squeeze casting, and PM were mostly used in fabricating the magnesium matrix composites reinforced by powders/fibers/whiskers. Some other processing techniques such as *in-situ* synthesis, mechanical alloying, pressureless infiltration, gas injection, and spray forming were also sometimes used. For magnesium matrix composites, the mechanical properties such as tensile strength, creep resistance, and fatigue resistance were improved, but at the cost of other properties, typically ductility. The poor ductility of magnesium matrix composites limits their widespread application.

Nanoparticle reinforcements can significantly increase the matrix mechanical strength by more effectively

G. CAO, Research Associate, J. KOBLSKA, Graduate Student, H. KONISHI, Research Associate, and X. LI, Associate Professor, are with Department of Mechanical Engineering, University of Wisconsin-Madison, Madison, WI 53706. Contact e-mail: xcli@engr.wisc.edu
Manuscript submitted June 13, 2007.

Article published online February 12, 2008

promoting particle hardening mechanisms than microparticles. A fine and uniform dispersion of nanoparticles provides a good balance between the strengthener (nondeforming particles, such as SiC nanoparticles) and interparticle spacing effects to maximize the yield strength and creep resistance. As predicted by an analytical model^[10] about metal matrix nanocomposites (MMNCs), the mechanical properties of metals would be enhanced considerably if reinforced by ceramic nanoparticles (less than 100 nm). Moreover, MMNCs could offer a significantly improved performance at elevated temperatures, because thermally stable ceramic nanoparticles can maintain their properties at high temperatures. The MMNCs are poised to generate enormous impact on aerospace, automobile, and military industries.

Solidification processing such as stir casting that used mechanical stirring was a widely used technique to produce magnesium matrix composites that were reinforced by microceramic particles. A combination of good distribution and dispersion of microparticles can be achieved by mechanical stirring. However, to produce magnesium matrix nanocomposites, it is extremely challenging for the conventional mechanical stirring method to distribute and disperse nanoparticles uniformly in metal melts because of the much higher specific surface areas in nanoparticles. In order to achieve a uniform dispersion and distribution of nanoparticles in magnesium matrix nanocomposites, Lan *et al.*,^[11] Li *et al.*,^[12] and Yang *et al.*^[13] developed a new technique that combined solidification processes with ultrasonic cavitation-based dispersion of nanoparticles in metal melts. It was reported^[14] that ultrasonic cavitation can produce transient (in the order of nanoseconds) micro “hot spots” that can have temperatures of about 5000 °C, pressures above 1000 atms, and heating and cooling rates above 10^{10} K/s. The strong impact coupling with local high temperatures can potentially break nanoparticle clusters and clean the particle surface. Because nanoparticle clusters are loosely packed together, air or vapor could be trapped inside the voids in the clusters, which will serve as nuclei for cavitations. The size of the clusters ranges from nano- to micrometers due to the attraction force among nanoparticles and the poor wettability between nanoparticles and metal melts.

In this article, a new class of magnesium matrix nanocomposites, namely, Mg-4Zn reinforced by SiC nanoparticles in this study, will be fabricated by ultrasonic cavitation-based solidification processing. The microstructure and overall mechanical properties of nanocomposites will be studied to understand the effect of nanoparticles in as-cast Mg alloys.

II. EXPERIMENTAL

Figure 1 shows the schematic experimental setup for the ultrasonic cavitation-based fabrication of SiC nanoparticle-reinforced magnesium matrix nanocomposites. It mainly consists of a resistance heating furnace for magnesium alloy melting, a nanoparticle feeding mechanism, a protection gas system, and an ultrasonic processing system. A mild steel crucible, which is 114 mm in inner diameter and 127 mm in height, was

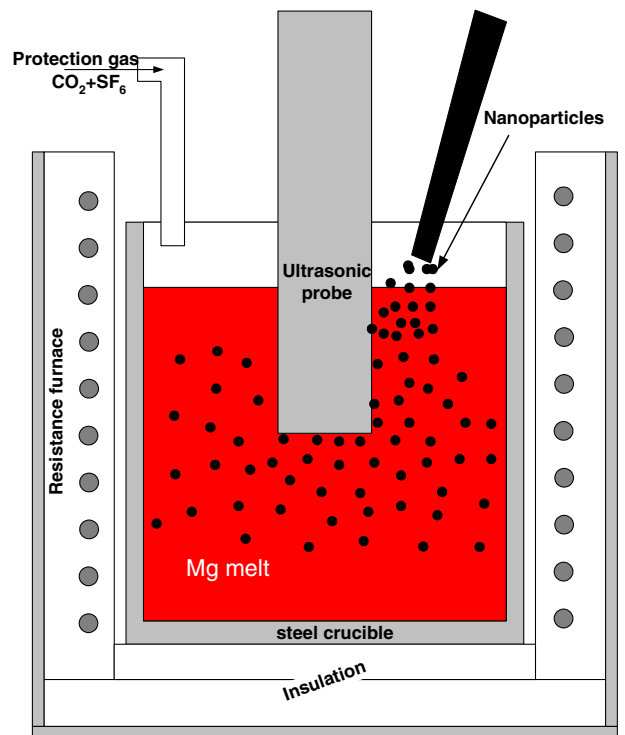


Fig. 1—Experimental setup for fabricating Mg-SiC nanocomposites.

used. A PermenDur power ultrasonic probe, made of niobium, was used to generate a 17.5 KHz ultrasonic wave with a maximum 4.0 kW power output (Advanced Sonics, LLC, Oxford, CT) for melt processing. The niobium probe is 32 mm in diameter and 102 mm in length. The ultrasonic probe was dipped into the melt for about 32 mm. The melt temperature for ultrasonic processing was controlled at about 700 °C. The SiC nanoparticles were fed into the Mg alloy melt through a steel tube. The average size of the SiC particles was about 50 nm. Figure 2(a) shows a transmission electron microscopy (TEM) image of SiC particles used in the experiments. The original powder was ultrasonicated in ethanol. A droplet of the resulting suspension was placed on a lacy C film and air dried. The particles were aggregated in many places. The average size of a particle is ~50 nm. Figure 2(b) shows an electron diffraction (ED) pattern of SiC nanoparticles. The SiC structure is cubic.

About 800 g of pure magnesium was first melted in the mild steel crucible; when the temperature of the melt reached 700 °C, pure Zn was added into the pure magnesium melt to make Mg-4Zn matrix. It should be noted that no Zr element, which is an effective grain refiner in Mg alloys that contain no Al or Mn, was added. It is expected that SiC nanoparticles can refine the grain size of Mg alloys significantly. The magnesium melt pool was protected by CO₂ + 0.75 pct SF₆. After processing, the magnesium melt was cast into a steel permanent mold (preheated to 350 °C). The mold was designed and fabricated according to ASTM B 108-03a. The pouring temperature was controlled at 745 °C. In each casting experiment, two standard tensile specimens, as shown in Figure 3, can be obtained. An additional graphite pouring cup was used to guide the melt and

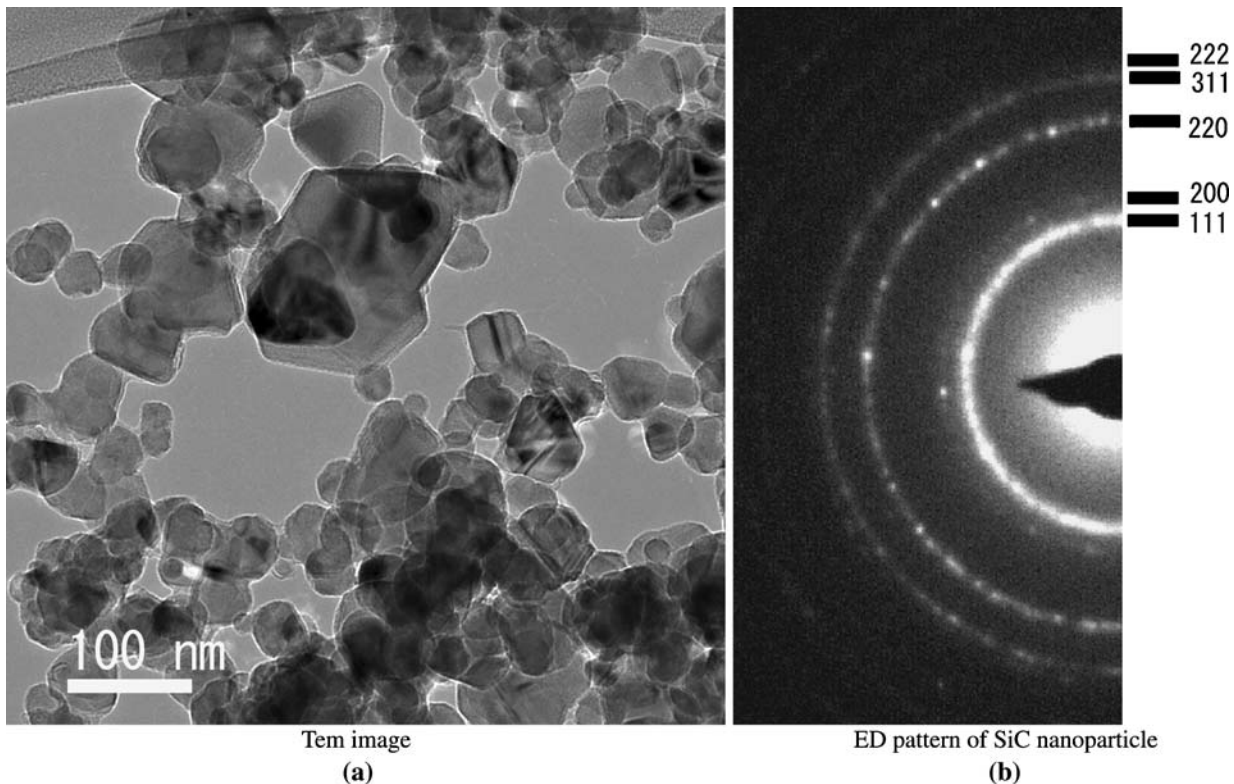


Fig. 2—SiC nanoparticles used in the experiments: (a) TEM image and (b) ED pattern of SiC nanoparticle.

serve as housing for the SiC ceramic filter, which has dimensions of 55 mm × 55 mm × 12 mm and a porosity per inch of 20 ppi.

To obtain mechanical properties of the Mg-4Zn/SiC nanocomposites, specimens with a diameter of 0.375 in. (9.5 mm) and a gage length of 1.75 in. (44.5 mm) were tested in a MTS Sintech 10/GL machine (MTS, Eden Prairie, MN). An extensometer with a 1-in. (25.4-mm) gage length is clamped to each tensile sample. The crosshead speed is set to 5 mm/min. When the strain reaches 1 pct, the tensile testing machine will pause temporarily so that the extensometer can be removed. At the first stage of tensile testing, the strain data comes from the extensometer. After the extensometer is removed, the tensile testing continues and the strain data comes only from the displacement reading of the tensile testing machine.

The microstructure of the samples was studied by optical microscopy, scanning electron microscopy (SEM), and TEM. The magnesium nanocomposite samples for optical microscopy and SEM were cut, mounted, mechanically ground, and polished. The SEM was conducted in a LEO 1530 machine (LEO Electron Microscopy Ltd., Thornwood, NY). TEM samples were prepared using ion milling. The TEM was conducted using a PHILIPS* CM 200UT microscope, operating at

*PHILIPS is a trademark of Philips Electronic Instruments Corp., Mahwah, NJ.

an accelerating voltage of 200 kV.

III. RESULTS AND DISCUSSION

Figure 4 shows the typical stress-strain curves of Mg-4Zn and Mg-4Zn/1.5 pct SiC nanocomposites. It should be mentioned that in the stress strain curves, there is a tiny kink at 1 pct strain, due to the removal of the extensometer. The average values of the tensile strength, yield strength, and ductility of the test samples are shown in Table I. The overall mechanical properties including tensile strength, yield strength, and ductility were improved significantly.

Figure 5 shows the optical microstructures of Mg-4Zn and Mg-4Zn/1.5 pct SiC nanocomposites. The samples were taken from a cross section at the end of the tensile bar gage section, which represents the true microstructure of the tensile bars well. As shown in the microstructure of Mg-4Zn, some porosity and even some large cracklike shrinkage areas exist. This is because the solidification range of Mg-4Zn is very wide as compared to other magnesium alloys such as AZ91D and Mg-Al alloys. The wide freezing range results in poor castability. Hence, a higher pouring temperature of 745 °C was used to cast Mg-4Zn, while the pouring temperature was only 725 °C for the casting of other alloys such as AZ91D. As shown in the microstructure of Mg-4Zn/1.5 pct SiC, some microclusters of SiC nanoparticles were still present. These clusters were distributed uniformly, but most were along the grain boundaries. It can also be seen that the grain size of Mg-4Zn was refined significantly by the addition of SiC nanoparticles. In as-cast Mg-4Zn, the average grain size was about 150 μm,

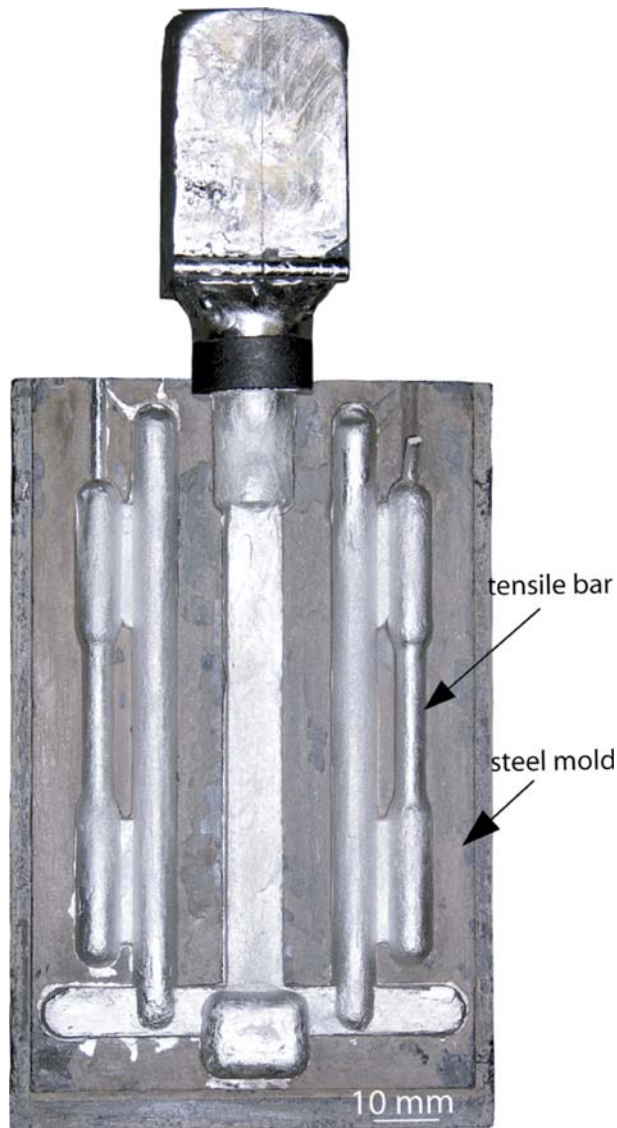


Fig. 3—Typical permanent mold casting samples for tensile testing.

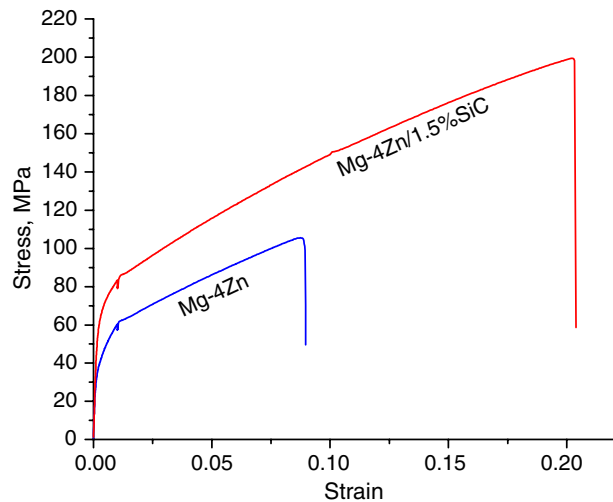


Fig. 4—Typical stress-strain curves of Mg-4Zn and Mg-4Zn/1.5 pct SiC nanocomposites.

Table I. Average Tensile Properties of the Mg-4Zn Matrix and Mg-4Zn/1.5 Pct SiC Nanocomposites

Materials	Yield Strength, MPa	Ultimate Tensile Strength, MPa	Ductility, Pct
Pure Mg-4Zn	41.5	105	8.5
Mg-4Zn/1.5 pct SiC	71.7	199.3	20.0

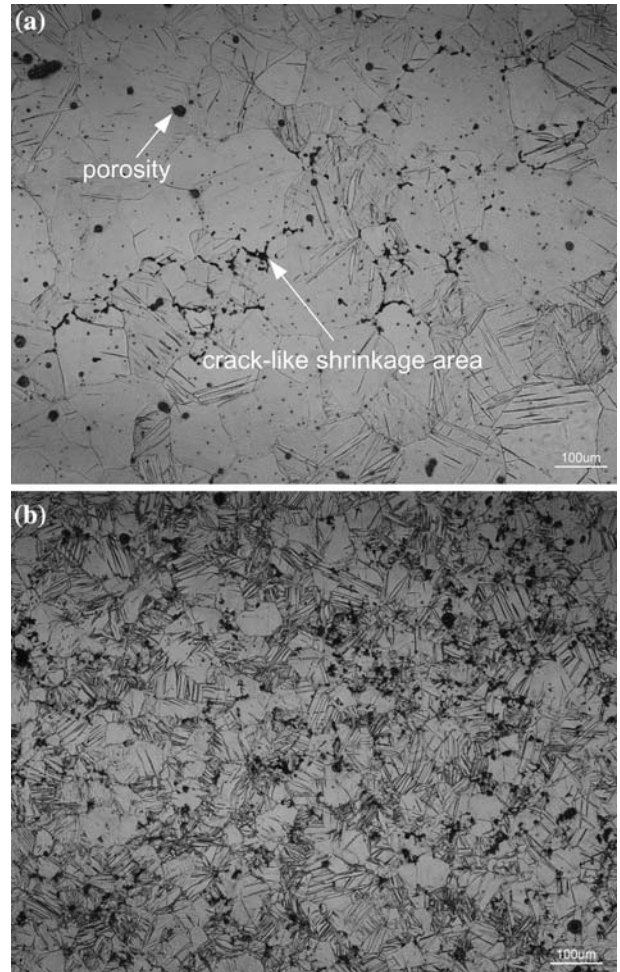


Fig. 5—Optical microstructures of (a) Mg-4Zn and (b) Mg-4Zn/1.5 pct SiC nanocomposites. Significant grain refining was achieved in Mg-4Zn/1.5 pct SiC nanocomposites, and shrinkage porosity was reduced.

while in as-cast Mg-4Zn/1.5 pct SiC nanocomposites, the average grain size was reduced to about 60 μm .

It is also worth mentioning that the castability of Mg-4Zn/1.5 pct SiC was also improved considerably. In as-cast Mg-4Zn, severe hot tearing occurred while little hot tearing existed in as-cast Mg-4Zn/1.5 pct SiC nanocomposites. The considerable improvement of the castability can also be attributed to the finer grain size in Mg-4Zn/1.5 pct SiC castings. Generally, the finer grain size can improve melt feeding characteristics, increase hot tearing resistance, and minimize shrinkage and porosity.

Figure 6(a) shows a low-magnification SEM image in the area with SiC microclusters in the Mg-4Zn/1.5 pct

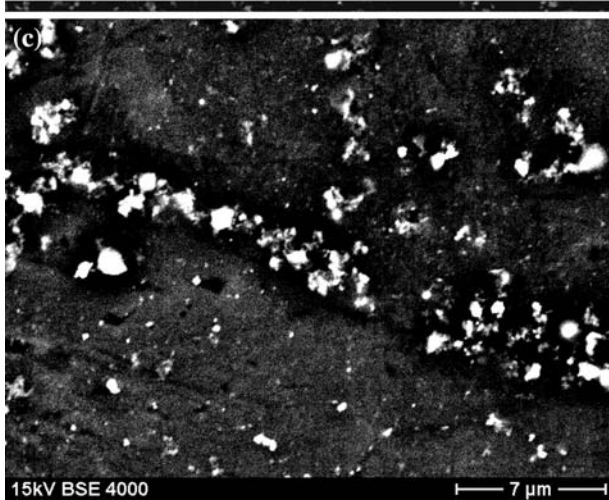
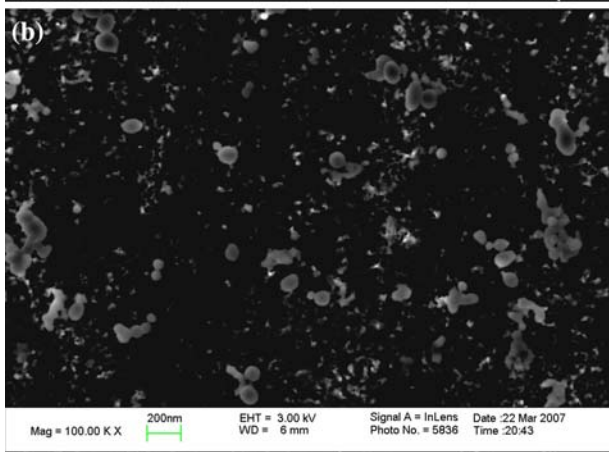
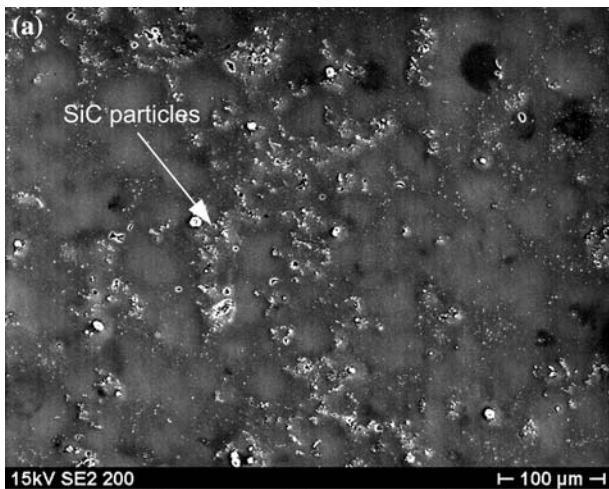


Fig. 6—SEM images of Mg-4Zn/1.5 pct SiC nanocomposites: (a) low magnification of an area full of SiC microcluster and (b) high magnification of an area outside the SiC microcluster areas. A good dispersion of SiC was achieved in Mg-4Zn/1.5 pct SiC nanocomposites. (c) High magnification of a typical cluster area.

SiC nanocomposites. From the optical images and low-magnification SEM images, there are still some SiC clusters. Although ultrasonic cavitation is quite effective in dispersing SiC nanoparticles, the processing parameters were still not optimized. Further improvement on the dispersion of nanoparticles is needed.

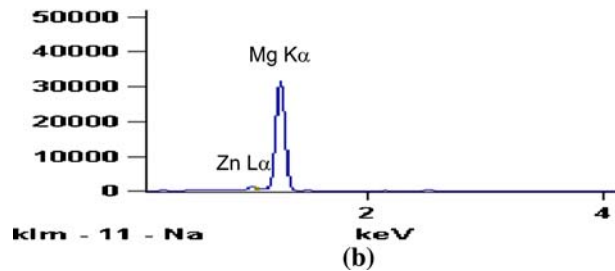
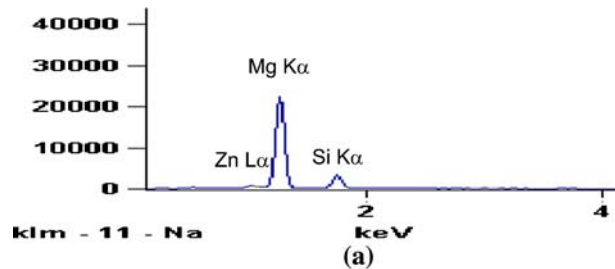


Fig. 7—EDS of Mg-4Zn/1.5 pct SiC nanocomposites: (a) clusters area and (b) Mg-4Zn matrix.

Figure 6(b) shows a higher magnification SEM image outside the area of SiC microclusters in the Mg-4Zn/1.5 pct SiC nanocomposites. It is clear that SiC nanoparticles were dispersed very well. Figure 6(c) shows an SEM image of a cluster area. It can be seen that microclusters are still separated to single nanoparticles or agglomerated nanoclusters. Figure 7 shows the EDS results from a SiC microcluster area and Mg-4Zn matrix. In Figure 7(a), the Si peak can be seen clearly, which indicates that the small clusters are SiC.

The significant improvement of mechanical properties and ductility in Mg-4Zn nanocomposites would mostly be attributed to the well-dispersed SiC nanoparticles. According to a recent published analytical model^[10] for predicting the yield strength of particulate-reinforced metal matrix nanocomposites, the strengthening of nanoparticles come from the Orowan strengthening effects, enhanced dislocation density, and load bearing effects. It is pointed out that Orowan strengthening is not significant in metal matrix composites enhanced by microparticles, but it becomes more favorable in metal matrix nanocomposites due to the fact that Orowan bowing is necessary for dislocations to bypass the nanoparticles. A small volume fraction of nanoparticles can significantly improve the yield strength of metal matrix nanocomposites. This is also a clear contrast to the magnesium matrix composites reinforced by microparticles or fibers, which contain 10 to 30 vol pct reinforcement phases.

From the low-magnification SEM and optical images, one would expect the ductility of Mg-4Zn/1.5 pct SiC nanocomposites to be reduced due to the existence of some microclusters. However, it is extremely interesting to note that the ductility of Mg-4Zn/1.5 pct SiC nanocomposites was actually increased significantly (from 8.5 to 20 pct). This possibly could be attributed to, at least, the following three aspects. First, although these SiC clusters appeared as microclusters, most of the nanoparticles in the microclusters

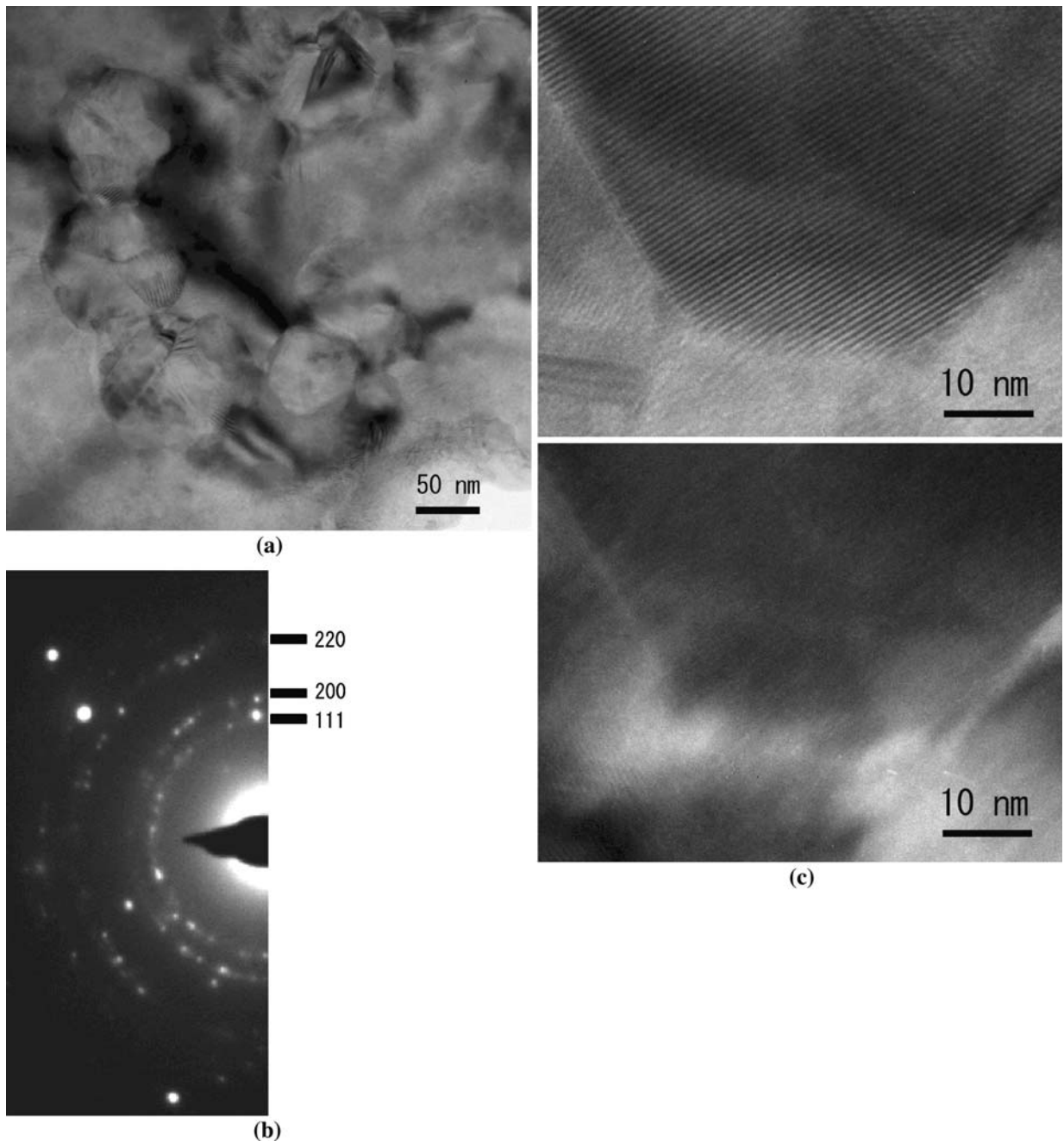


Fig. 8—TEM image of SiC particles in Mg-4Zn magnesium alloy matrix. (a) Low-magnification image of SiC nanoclusters and single particles in a microcluster area. Strain contrast appears near the interface in some places. (b) ED patterns from SiC particles. (c) Moiré fringes of SiC in the Mg-4Zn magnesium alloy (top) and the 100 dark-field image of Mg-4Zn magnesium alloy (bottom).

are still separated to single nanoparticles or sintered nanoclusters, as shown in Figure 6(c). Second, the negative effects of some SiC microclusters were balanced by the positive effects of the grain refining effects and strengthening effects of the well-dispersed SiC nanoparticles. Third, the improvement of ductility in Mg-4Zn/1.5 pct SiC nanocomposites can also be partly attributed to the decreasing of porosity and cracklike shrinkage areas in Mg-4Zn. Because of the wide freezing temperature range of Mg-4Zn, quite some porosity and cracklike shrinkage areas formed at the

end of solidification. These porosity and cracklike shrinkage areas are detrimental to the ductility. However, this is the first time in our study to show this significant ductility-enhancing effect for as-cast Mg matrix nanocomposites. Normally, the ductility of as-cast magnesium nanocomposites (*e.g.*, pure Mg reinforced by SiC nanoparticles) were only retained.^[12] Therefore, the mechanism for this significant improvement in ductility needs further fundamental study.

As shown in Figure 8(a), some SiC nanoclusters existed in a microcluster area, suggesting most

nanoparticles were dispersed well even in the areas of microclusters. As shown in Figure 8(b), the crystal structures of SiC are cubic, and they have a random orientation in the Mg-4Zn magnesium alloy matrix. In Figure 8(c), clear Moire fringes (~0.8 nm) of SiC in Mg-4Zn magnesium alloy were observed in the SiC nanoparticle, suggesting that no intermediate phase occurs. In some cases, strain contrast was observed near the interface, indicating that SiC is bonded to Mg-4Zn magnesium alloy (Figures 8(a) and (c)).

IV. SUMMARY

Ultrasonic cavitation is an effective way to disperse SiC nanopowders in the Mg-4Zn melt for solidification processing of Mg-4Zn/SiC nanocomposites. However, some SiC microclusters still existed in the Mg-4Zn/1.5 pct SiC microstructure. With the addition of SiC nanoparticles, the grain size of magnesium was refined significantly. The castability of Mg-4Zn/1.5 pct SiC was also improved, as compared to that of Mg-4Zn matrix. The TEM study indicates that SiC nanoparticles bond well with Mg-4Zn magnesium alloy without forming an intermediate phase. The ultimate tensile strength and yield strength were increased significantly. The ductility of Mg-4Zn/1.5 pct SiC was more than 2 times that of unenhanced Mg-4Zn. While the mechanism for this ductility enhancement is not well understood, it is certainly of interest to academia and industries for further fundamental study.

ACKNOWLEDGMENT

This work was supported by the National Science Foundation (Grant No. 0506767).

REFERENCES

1. Y.L. Xi, D.L. Chai, W.X. Zhang, and J.E. Zhou: *Mater. Lett.*, 2005, vol. 59, pp. 1831–35.
2. Y.L. Xi, D.L. Chai, W.X. Zhang, and J.E. Zhou: *Rare Met. Mater. Eng.*, 2005, vol. 34, pp. 1131–34.
3. S.B. Li, W. Gan, M. Zheng, and K. Wu: *Trans. Nonferrous Metals Society of China*, 2005, vol. 15, pp. 245–50.
4. O. Hideki, K. Katsuyoshi, S. Masaki, and Y. Eiji: *J. Jpn. Soc. Powder Metall.*, 2005, vol. 52, pp. 282–86.
5. Q.C. Jiang, H.Y. Wang, B.X. Ma, Y. Wang, and F. Zhao: *J. Alloys Compd.*, 2005, vol. 386, pp. 177–81.
6. Y. Zhang, Y. Xue, S. Li, J. Huang, and C. Huang: *Mater. Sci. Forum*, 2005, vols. 488–489, pp. 897–900.
7. B.X. Ma, H.Y. Wang, Y. Wang, and Q.C. Jiang: *J. Mater. Sci.*, 2005, vol. 40, pp. 4501–04.
8. M. Pahutova, V. Sklenicka, K. Kucharova, and M. Svoboda: *Int. J. Mater. Product Technol.*, 2003, vol. 18, pp. 116–40.
9. H.Z. Ye and X.Y. Liu: *J. Mater. Sci.*, 2004, vol. 39, pp. 6153–71.
10. Z. Zhang and D.L. Chen: *Scripta Mater.*, 2006, vol. 54, pp. 1321–26.
11. J. Lan, Y. Yang, and X. Li: *Mater. Sci. Eng. A*, 2004, vol. 386, pp. 284–90.
12. X. Li, Z. Duan, G. Cao, and A. Roure: *Trans. Am. Foundry Soc.*, 2007, vol. 115, pp. 747–52.
13. Y. Yang and X. Li: *ASME J. Manufact. Sci. Eng.*, 2007, vol. 129, pp. 252–55.
14. K.S. Suslick, Y. Didenko, M.M. Fang, T. Hyeon, K.J. Kolbeck, W.B. McNamara, M.M. Mdeleleni, and M. Wong: *Phil. Trans. Roy. Soc. A*, 1999, vol. 357, pp. 335–53.